Carcinogenesis vol.34 no.11 pp.2486–2497, 2013
doi:10.1093/carcin/bgt240
Advance Access publication July 3, 2013

Curcumin suppresses multiple DNA damage response pathways and has potency as a sensitizer to PARP inhibitor

Hideaki Ogiwara, Ayako Ui[1], Bunsyo Shiotani[2,3], Lee Zou[2], Akira Yasui[1] and Takashi Kohno*

Division of Genome Biology, National Cancer Center Research Institute, Tokyo 104-0045, Japan, [1]Department of Molecular Genetics, Institute of Development, Division of Dynamic Proteome, Aging and Cancer, Tohoku University, Sendai 980-8575, Japan and [2]Massachusetts General Hospital Cancer Center, Harvard Medical School, Charlestown, MA 02129, USA
[3]Present address: Department of Cellular and Molecular Biology, Graduate School of Biomedical Science, Hiroshima University, Hiroshima 739-0046, Japan

*To whom correspondence should be addressed. Division of Genome Biology, National Cancer Center Research Institute, 5-1-1 Tsukiji, Chuo-ku, Tokyo 104-0045, Japan. Tel: +81 3 3542 2511; Fax: +81 3 3542 0807; Email: tkkohno@ncc.go.jp

Inhibitors of poly(ADP-ribose) polymerase (PARP) are promising anticancer drugs, particularly for the treatment of tumors deficient in the DNA damage response (DDR). However, it is challenging to design effective therapeutic strategies for use of these compounds against cancers without DDR deficiencies. In this context, combination therapies in which PARP inhibitors are used alongside DDR inhibitors have elicited a great deal of interest. Curcumin, a component of turmeric (*Curcuma longa*), has been tested in clinical studies for its chemosensitizing potential; however, the mechanisms of chemosensitization by curcumin have not been fully elucidated. This study demonstrates that curcumin suppresses three major DDR pathways: non-homologous end joining (NHEJ), homologous recombination (HR) and the DNA damage checkpoint. Curcumin suppresses the histone acetylation at DNA double-strand break (DSB) sites by inhibiting histone acetyltransferase activity, thereby reducing recruitment of the key NHEJ factor KU70/KU80 to DSB sites. Curcumin also suppresses HR by reducing expression of the *BRCA1* gene, which regulates HR, by impairing histone acetylation at the *BRCA1* promoter. Curcumin also inhibits ataxia telangiectasia and Rad3-related protein (ATR) kinase (IC_{50} *in vitro* = 493 nM), resulting in impaired activation of ATR-CHK1 signaling, which is necessary for HR and the DNA damage checkpoint pathway. Thus, curcumin suppresses three DDR pathways by inhibiting histone acetyltransferases and ATR. Concordantly, curcumin sensitizes cancer cells to PARP inhibitors by enhancing apoptosis and mitotic catastrophe via inhibition of both the DNA damage checkpoint and DSB repair. Our results indicate that curcumin is a promising sensitizer for PARP inhibitor-based therapy.

Introduction

Poly(ADP-ribose) polymerase (PARP) inhibitors are a promising new class of anticancer drugs that inhibit the enzymatic activity of PARP1 protein, which is involved in the repair of DNA single-strand breaks (SSBs) (1). Inhibition of PARP1 impairs SSB repair and increases the number of DNA double-strand breaks (DSBs) (1). Cancer cells that lack intact BRCA1 or BRCA2 protein, exemplified by hereditary breast and ovarian cancers, are deficient in the DNA damage response (DDR) (2–5). Several clinical trials have demonstrated that PARP inhibitors are highly effective at killing such cancers (6–10). Inhibition of PARP activity is also detrimental to cancer cells whose DDR activities are deficient due to RNAi-mediated ablation of DDR genes other than BRCA1/2 (5,11). However, most human cancers contain intact DDR genes and retain DDR activity. Therefore, it will be challenging, but is nonetheless essential, to establish effective therapeutic methods for using PARP inhibitors against the majority of cancers, which lack DDR deficiencies. In such efforts, drugs that inhibit protein(s) required for DDR pathways will be used to potentiate the effect of PARP inhibitors.

Three DDR pathways, including homologous recombination (HR), non-homologous end joining (NHEJ) and the DNA damage checkpoint, play important roles in allowing cancer cells to survive genotoxic events caused by treatment with PARP inhibitors. Two of these pathways are major systems devoted to the repair of DSBs: NHEJ joins broken DNA ends without requiring extensive sequence homology, whereas HR uses long stretches of homologous sequence (12–14). The third pathway is the DNA damage checkpoint, which arrests the cell cycle in the presence of DNA damage (15).

The fundamental steps of NHEJ, synapsis and ligation, employ KU80/DNA-PK_{CS} and LIG4-XRCC4-XLF, respectively (11,12,14,16–20). However, histone modification and chromatin remodeling are also required to relax chromatin and permit recruitment of NHEJ factors (21,22). Histone acetylation at DSB sites by the histone acetyltransferases (HATs) CBP, p300 and GCN5 is a critical step that allows accumulation of the SWI/SNF chromatin remodeling complex, which opens chromatin structure and thereby grants access to NHEJ factors (22,23).

The HR pathway, on the other hand, restores the genomic sequence at a DSB by utilizing the sister chromatid as a template for repair (24). In HR, DSBs are first recognized by the MRE11-RAD50-NBS1 (MRN) complex, which is then activated by CtIP and BRCA1 (25,26). Next, the DNA ends are resected by the MRN complex to allow accumulation of replication protein A (RPA) (RPA70/RPA32/RPA16) (27). Assembly of RAD51 on RPA-coated single-stranded DNA (RPA-ssDNA) leads to HR (28). RPA-ssDNA activates ataxia telangiectasia and Rad3-related protein (ATR), leading to phosphorylation of CHK1 kinase, which in turn phosphorylates RAD51 and thereby promotes RAD51 recruitment to damaged sites. Thus, ATR-CHK1 signaling positively regulates the HR pathway (29,30).

DSBs also cause the activation of the ATR-CHK1 and ATM-CHK2 DNA damage checkpoint pathways, which arrest the cell cycle to allow sufficient time for DNA repair to take place (31,32). Inhibition of the DNA damage checkpoint abrogates cell cycle arrest, leading to mitotic catastrophe and apoptosis while mostly sparing non-cancerous cells. This effect appears to be stronger in some cancer cells than in non-cancer cells, presumably because the more sensitive cancer cells contain unspecified abnormalities in DDR pathways (33–36).

Effective sensitization to PARP inhibitor-based therapy could be achieved by inhibiting any of these three DDR pathways (37). To this end, one could use PARP inhibitors in combination with compounds that effectively inhibit DDR and ideally exert minimal toxicity in the human body. Curcumin (diferuloylmethane) is a yellow pigment contained in Indian saffron (*Curcuma longa*; turmeric) and has been traditionally used as a foodstuff, cosmetic and medicine. In addition, curcumin can inhibit a variety of enzymes, including HATs (35). Because it is non-toxic even at high doses, curcumin has been intensively tested in both preclinical and clinical trials for its chemopreventive potential in a variety of diseases, including cancer (35). In addition, recent clinical studies indicate that curcumin is potentially useful as a sensitizer in gemcitabine chemotherapy against

Abbreviations: ATM, ataxia telangiectasia mutated; ATR, ataxia telangiectasia and Rad3-related protein; ATRIP, ATR interacting protein; BB, blocking buffer; ChIP, chromatin immunoprecipitation; CPT, camptothecin; DDR, DNA damage response; DMSO, dimethyl sulfoxide; DSB, double-strand break; GFP, green fluorescent protein; HAT, histone acetyltransferase; HR, homologous recombination; HU, hydroxyurea; IR, ionizing radiation; NCS, neocarzinostatin; NF-κB, nuclear factor-kappaB; NHEJ, non-homologous end joining; PARP, poly(ADP-ribose) polymerase; PI, propidium iodide; PBS, phosphate-buffered saline; RPA, replication protein A; siRNA, small interfering RNA; SSB, single-strand break; ssDNA, single-stranded DNA.

advanced pancreatic cancers (38,39). One candidate mechanism for the chemosensitizing effect of curcumin in cancer cells is suppression of the antiapoptotic nuclear factor-kappaB (NF-κB) pathway through inhibition of IKKβ, an activator of NF-κB (40,41). IKKβ is involved in the repair of ionizing radiation (IR)-induced DSBs, and several other targets of curcumin, including AKT1 (37) and CBP/p300 (42), are also involved in the DDR. AKT1 interacts with and activates a NHEJ key factor, DNA-PK$_{CS}$ (43–45). We recently showed that CBP and p300 promote NHEJ, HR and the DNA damage checkpoint via histone acetylation at DSB sites and the promoter regions of genes encoding two key HR factors, BRCA1 and RAD51 (22,46). Thus, because it could potentially suppress multiple DDRs in cancer cells, curcumin is a strong candidate for an agent that could sensitize cancer cells to PARP inhibitors; however, this possibility has not yet been investigated.

Here, we show that curcumin inhibits NHEJ and HR by suppressing histone acetylation at DSB sites, as well as by suppressing transcription of the *BRCA1* gene through histone acetylation at its promoter region, as predicted from its inhibition of CBP and p300. In addition, we report a novel activity for curcumin, inhibition of ATR kinase, which results in impaired activation of ATR-CHK1 signaling. Because curcumin can simultaneously suppress two major DSB repair pathways, NHEJ and HR, as well as the ATR-CHK1 DNA damage checkpoint pathway, it holds promise as a sensitizer for PARP inhibitor-based cancer therapy.

Materials and methods

Materials

HeLa (cervical cancer), U2OS (osteosarcoma), HT1080 (fibrosarcoma) and HCT116 (colorectal cancer) cells were cultured in Dulbecco's modified Eagle's medium supplemented with 10% fetal bovine serum. H1299 (non-small-cell lung carcinoma) cells were cultured in RPMI-1640 supplemented with 10% fetal bovine serum. These cell lines were used as representatives of cancers that do not have DDR deficiency as a result of BRCA1/2 mutations. The chemical agents used in this study were as follows: curcumin (Sigma: ≥94% curcuminoid content; Sabinsa: ≥95% curcuminoid content) and olaparib (Selleck). Curcumin from Sabinsa was used only for experiments to address effects on phosphorylation on checkpoint-related proteins (Figure 4A).

Irradiation

Irradiation was performed using a ^{60}Co γ-ray source (Atomic Energy of Canada, Ontario, Canada) at a dose rate of 9.1 Gy/min.

Immunofluorescence microscopy

Cells were grown on glass cover slips, fixed with 2% (wt/vol) paraformaldehyde in phosphate-buffered saline (PBS) for 15 min at room temperature and then permeabilized with 0.3% (vol/vol) Triton X-100 for 15 min at room temperature. After fixation, cells were washed three times with PBS and then blocked with blocking buffer (BB: 1% bovine serum albumin, 0.1% Triton X-100 in PBS) for 10 min. Cells were incubated with primary antibody (diluted in BB) for 1 h at room temperature, washed with PBS and then incubated for 1 h at room temperature with Alexa Fluor 488-conjugated goat anti-mouse, Alexa Fluor 488-conjugated goat anti-rabbit, Alexa Fluor 568-conjugated goat anti-mouse or Alexa Fluor 568-conjugated goat anti-rabbit secondary antibodies (Molecular Probes) diluted in BB. Cells were then washed three times with PBS and counter-stained with 4′,6-diamidino-2-phenylindole (0.4 μg/ml in PBS) to visualize DNA. The cover slips were mounted onto glass slides using Prolong Gold mounting agent (Invitrogen). Confocal images were taken using an inverted microscope (Carl Zeiss) equipped with a ×100 oil lens. Images were acquired using the ZEN Software 2008 (Carl Zeiss). All immunofluorescence experiments were repeated at least twice, and representative images are shown. The percentage of foci-positive cells was determined from >100 cells per sample, and each of these experiments was performed in triplicate.

In vitro *kinase assays*

The ATR kinase assays were performed essentially as described previously (47), with the following modifications. To analyze the inhibitory effect of curcumin, the ATR-ATRIP (ATR interacting protein) complex was purified using a two-step protocol. HEK 293E cells were transfected with FLAG-ATR- and His-ATRIP-expressing plasmids, and the ATR-ATRIP complex was purified using Ni-beads followed by elution with imidazole. Proteins eluted from the Ni-beads were subsequently incubated with anti-FLAG M2 beads, and the ATR-ATRIP complex was eluted with 200 μg/ml 3 × FLAG peptide. The kinase reactions were performed using purified ATR-ATRIP complex, GST-Rad17 and 10 μCi [γ-^{32}P]ATP in the presence or absence of curcumin. The concentration of curcumin that achieved 50% inhibition of the enzyme (IC_{50}) was derived from log approximation plots. Enzyme activity was plotted against curcumin concentration. Data represent the means ± SD of three independent experiments.

DNA damage checkpoint analysis

Cells were exposed to 2 Gy IR from a ^{60}Co source after exposure to the indicated agents for 1 h. Cells were harvested 1 h after IR exposure, washed twice with ice-cold PBS, fixed, permeabilized with 70% ethanol and stored at −20°C for at least 2 h. Fixed cells were blocked with BB (0.5% bovine serum albumin in PBS) for 10 min at room temperature. Cells were then stained for 1 h at room temperature with an anti-phospho-histone H3 (Ser10) antibody diluted 1:25 in BB. Washes were carried out three times in PBS. For secondary staining, cells were incubated for 1 h at room temperature with fluorescein-isothiocyanate-conjugated donkey anti-mouse IgG antibody (Jackson ImmunoResearch), diluted 1:100 in BB. After secondary antibody staining, cells were washed three times, incubated with 5 μg/ml propidium iodide (PI) and 200 μg/ml RNase I in PBS and analyzed using a Guava flow cytometer. The resulting data were analyzed using the GuavaSoft 2.2 software.

Survival assays

For clonogenic assays, cells were trypsinized, counted and plated in six-well dishes (500–1000 cells/dish). Cells were incubated for 6 h before drug treatment. Following a 14 day recovery and growth period, colonies were fixed in a 50% (vol/vol) methanol/0.01% (wt/vol) crystal violet solution for 5 min. Survival points were assayed in triplicate, and data are shown as the means ± SD. Cell viability was determined by assessing cellular adenosine triphosphate levels using a CellTiter-Glo kit (Promega Corporation, Madison, WI).

Statistical analysis

Drug-treatment experiments were performed in triplicate. Data are shown as the means ± SD. Differences between drug-treated and untreated cells were evaluated by Student's *t*-test, and statistical differences are indicated by asterisks (*$P < 0.05$; **$P < 0.01$; ***$P < 0.001$; and ****$P < 0.0001$).

Other methods are described in Supplementary Materials and methods, available at *Carcinogenesis* Online.

Results

Curcumin suppresses NHEJ by suppressing histone acetylation at DSB sites

Curcumin acts as a chemo- and radiosensitizer (39), suggesting that it suppresses DSB repair; however, the underlying mechanisms are unknown. We first examined the effects of curcumin on the repair of IR-induced DSBs using a neutral comet assay, which specifically detects DSBs. Curcumin impaired the repair of IR-induced DSBs in HeLa cells in a concentration-dependent manner (Figure 1A and B). Next, we investigated whether NHEJ can be suppressed by curcumin (Figure 1C) using an NHEJ assay we developed previously (22). Treatment of H1299dA3-1 cells with either curcumin or NU7026, an inhibitor of the key NHEJ factor DNA-PK$_{CS}$, led to a reduction in the proportion of enhanced green fluorescent protein (GFP)-positive cells (Figure 1D), indicating that curcumin has the ability to suppress NHEJ.

Recently, we revealed that CBP and p300, two HATs targeted by curcumin (48), acetylate histones near DSB sites and are required for efficient DSB repair (22). In light of this finding, we investigated the impact of curcumin treatment on histone acetylation induced by I-*Sce*I-mediated DSBs. Chromatin immunoprecipitation (ChIP) assays revealed that the acetylation levels of histone H3 K18 near the I-*Sce*I site decreased upon treatment with curcumin (Figure 1E). In addition, curcumin treatment led to a reduction in recruitment of the key NHEJ factors KU70 and KU80 to DSB sites induced by I-*Sce*I or laser microirradiation (Figure 1F–H). Consistent with this, IR-induced phosphorylation of DNA-PK$_{CS}$, which is dependent on KU70/KU80 binding at DSB ends, was suppressed by treatment with curcumin (Figure 1I), as well as by knockdown of CBP or p300 (data

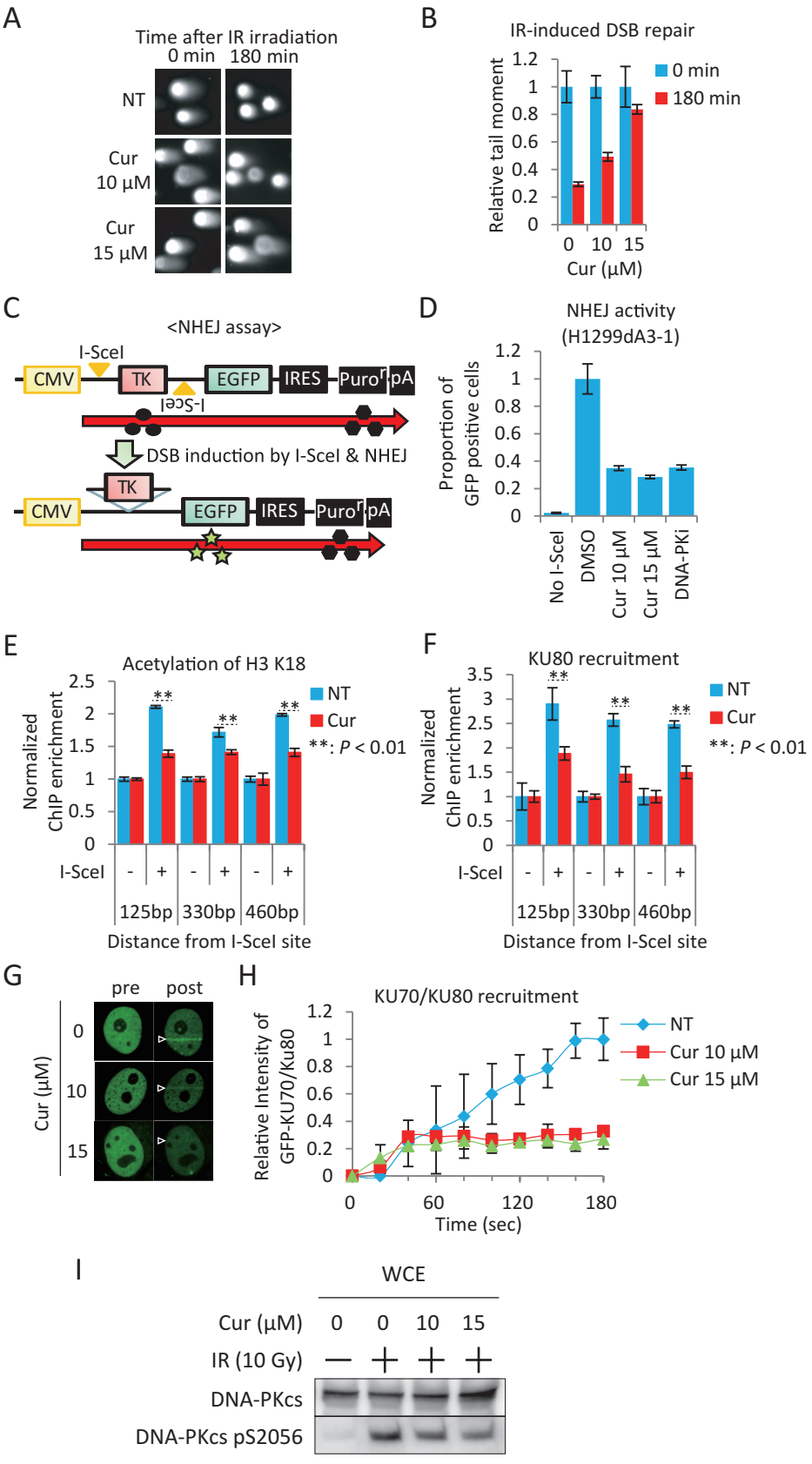

Fig. 1. Treatment with curcumin suppresses NHEJ by inhibiting histone H3/H4 acetylation and KU70/KU80 recruitment at DSB sites. (**A** and **B**) Suppression of IR-induced DSB repair by curcumin. HeLa cells were treated with 0 μM (NT) or 10 or 15 μM curcumin (Cur), and 1 h later were exposed to 20 Gy IR and subjected to neutral comet analyses at the indicated time points. (A) Representative comet images. (B) Efficiency of DSB repair. Comet tail moment (% DNA in tail × tail length) is expressed as the mean ± SD of triplicate experiments. (**C** and **D**) Suppression of NHEJ by treatment with curcumin and AKT inhibitors. (C) NHEJ assay system in H1299dA3-1 cells. Two *I-Sce*I sites in opposite orientations are indicated by yellow arrowheads. CMV, cytomegalovirus promoter/enhancer; IRES, internal ribosome entry site; PA, poly-A signal. (D) NHEJ activity following treatment with inhibitors. H1299dA3-1 cells were transfected

not shown). Neither curcumin treatment nor small interfering RNA (siRNA)-mediated knockdown of CBP and p300 affected the expression level of core NHEJ factors (data not shown) (22). These observations implied that curcumin suppresses NHEJ by inhibiting the HAT activities of CBP and p300.

Treatment with specific inhibitors of AKT, a target of curcumin that may be involved in NHEJ (44,45,49), also led to a reduction in the proportion of enhanced GFP-positive cells (Supplementary Figure S1A, available at *Carcinogenesis* Online). A similar reduction was observed when AKT1 was knocked down using siRNA (Supplementary Figure S1B and C, available at *Carcinogenesis* Online). However, treatment of curcumin at a concentration that suppresses NHEJ *in vivo* did not inhibit phosphorylation of AKT (i.e. AKT activation) in response to IR, although treatment with inhibitors of DNA-PK_{CS} or AKT did reduce AKT activation (Supplementary Figure S1D, available at *Carcinogenesis* Online). Another target of curcumin, IKKβ, is also involved in the repair of IR-induced DNA damage. Treating cells with the specific IKKβ inhibitor BMS-345541 (IKKi III), at or above the concentration that reduces cell growth by 50% (IG_{50}; Supplementary Figure S1E, available at *Carcinogenesis* Online), did not significantly suppress NHEJ activity (Supplementary Figure S1A, available at *Carcinogenesis* Online). Together, these results strongly suggest that suppression of NHEJ by curcumin results from inhibition of CBP and p300.

Curcumin suppresses HR by transcriptional suppression of BRCA1

We next investigated the impact of curcumin treatment on HR of DSBs using an *in vivo* GFP-based chromosomal assay. In the DR-GFP assay, a DSB is generated by expression of the I-*Sce*I endonuclease, whose recognition site is integrated in the *GFP* gene such that digestion disrupts the gene and HR restores the intact *GFP* gene (Figure 2A) (50). Curcumin treatment reduced the proportion of GFP-positive cells, as did treatment with KU55933, a specific inhibitor of ataxia telangiectasia mutated (ATM), which is required for the activation of several HR-related factors (42,51) (Figure 2B). The proportion of repaired products, but not the proportion of cut products, was reduced by treatment with curcumin (Figure 2C and D; Supplementary Figure S2, available at *Carcinogenesis* Online), indicating that curcumin inhibits HR activity but neither DSB generation nor GFP transcription.

We recently revealed that double knockdown of CBP and p300 causes downregulation of *BRCA1* expression by suppressing histone acetylation and recruitment of the E2F1 transcription factor to the *BRCA1* promoter region (46). BRCA1 contributes to DNA end resection at DSBs as a component of the BRCA1-CtIP-MRN complex. This complex promotes RPA phosphorylation, leading to the binding of phosphorylated RPA and RAD51 to ssDNA and ultimately to formation of RAD51/RPA foci that undergo HR (25,26). Treatment with curcumin for 24 h led to the downregulation of BRCA1 protein and mRNA levels in HeLa and H1299 cells (Figure 2E and F). As in the case of siRNA-mediated CBP/p300 knockdown (46), curcumin treatment reduced the acetylation levels of histone H3 and the localization of E2F1 at the *BRCA1* promoter region (Figure 2G; Supplementary Figure S3, available at *Carcinogenesis* Online). *BRCA1* transcription levels change during the cell cycle: they are low in G_0/G_1 phase and high in the S and G_2 phases (23,52). However, curcumin treatment increased the population of cells in S and G_2/M but not in G_1 (Supplementary Figure S4, available at *Carcinogenesis* Online). Therefore, the decrease in *BRCA1* expression was not due to cell cycle changes but was instead likely to be due to the suppression of histone acetylation at the *BRCA1* promoter region.

BRCA1 regulates the recruitment of RPA to DSB sites by promoting resection of DNA ends (25,53). We recently showed that siRNA-mediated knockdown of CBP or p300, which causes a reduction in *BRCA1* expression, suppresses the recruitment of RPA to DSB sites (46). Consistent with this, curcumin treatment for 24 h also impaired the neocarzinostatin (NCS)-induced phosphorylation of RPA32 in both HeLa and H1299 cells (Figure 2H). Together, these data indicate that curcumin suppresses HR by downregulating the transcription of *BRCA1*.

Curcumin suppresses HR and the DNA damage checkpoint by inhibiting ATR kinase

In contrast to the long-term (24 h) treatment described above, short-term (1 h) treatment with curcumin did not affect the NCS-induced phosphorylation of RPA32 (Figure 3A), the proportion of cells positive for IR- or camptothecin (CPT)-induced RPA32/53BP1 foci (Figure 3B–D, Supplementary Figure S5A and B, available at *Carcinogenesis* Online) or the formation of IR-induced BRCA1 foci (Supplementary Figure S5C, available at *Carcinogenesis* Online). On the other hand, the proportion of cells containing IR-induced RAD51 foci was considerably reduced by short-term treatment with curcumin (Figure 4E; Supplementary Figure S5D, available at *Carcinogenesis* Online). These results led us to hypothesize that curcumin inhibits targets other than CBP/p300 HATs. CPT and hydroxyurea (HU) cause DSBs during DNA replication in S phase by inducing collapse of replication forks, and the resulting DSBs undergo HR (54). Consistent with this, >90% of CPT- or HU-treated cells containing pan-nuclear γH2AX foci also contained RAD51 foci; however, the proportion of such cells significantly decreased following treatment with curcumin (Figure 3F; Supplementary Figure S5E, available at *Carcinogenesis* Online). Curcumin also decreased the elevation in the amount of RAD51, but not of RPA32 and RPA70, in the chromatin-enriched fraction following IR treatment (Figure 3G). These results suggest that curcumin has the additional ability to suppress RAD51 assembly, irrespective of DNA end resection.

RAD51 assembly on damaged chromatin requires ATR-CHK1 signaling in response to the formation of RPA-coated ssDNA: ATR kinase activates CHK1 by phosphorylating CHK1 at Ser345, and activated CHK1 enhances RAD51 assembly and the HR reaction (29). Therefore, we next investigated whether curcumin suppresses CHK1 phosphorylation induced by DNA damage. IR-induced CHK1 phosphorylation was impaired by treatment with curcumin (Figure 4A),

←
with I-*Sce*I expression plasmid and harvested 48 h after transfection. The proportion of enhanced GFP-positive cells after treatment with the indicated inhibitors is expressed as a ratio relative to the proportion in the non-treated (NT) sample. The results are presented by the means ± SD of triplicate experiments. (**E** and **F**) Curcumin suppressed histone acetylation and KU80 recruitment at I-*Sce*I-induced DSB sites. After H1299dA3-1 cells were pretreated with 0 μM (NT) or 10 μM curcumin (Cur) for 30 min, cells were subsequently treated with 0 μM (NT) or 10 μM curcumin (Cur) and then subjected to ChIP assay 0 h (–) and/or 18 h (+) after being transfected with the I-*Sce*I expression plasmid. DNAs immunoprecipitated with antibodies against acetylated H3 K18 (H3 AceK18) (E) or KU80 (F) were subjected to quantitative PCR for regions 125, 330 and 460 bp from the I-*Sce*I site. The ChIP enrichment of proteins at DSBs after 18 h (+), normalized against the value at 0 h (–), is shown. Data represent the means ± SD. Each experiment was performed in triplicate, and the results are shown as the means ± SD. Asterisks indicates statistically significant differences between curcumin-treated and untreated cells, as determined by Student's *t*-test (**$P < 0.01$). (**G** and **H**) Curcumin suppressed KU70/KU80 recruitment at microirradiation-induced DSB sites. H1299 cells were transfected with both plasmids for the expression of GFP-KU70 and GFP-KU80 and treated with curcumin for 1 h. The cells were examined at the indicated time points after 405 nm laser microirradiation at a dose of 800 mW (500 scans at 1.6 mW/scan). At least 1000 DSBs were produced in each cell. (**G**) Representative fields for GFP-KU70/KU80 120 s after laser microirradiation. (**H**) Real-time recruitment of GFP-KU70/KU80. The GFP-KU70/KU80 fluorescence intensities at laser microirradiation sites at the indicated times, relative to the value in the NT sample after 180 s, are shown. Data represent the means ± SD. For evaluation of accumulation and kinetics, the mean intensity of irradiated regions was obtained after subtraction of the background intensity in the irradiated cell, and mean values of at least three independent experiments are given. (**I**) Impairment of IR-induced DNA-PK_{CS} activation by curcumin treatment. HeLa cells treated with control (NT) or 10 or 15 μM curcumin (Cur) for 1 h were subjected to 0 (–) or 10 Gy (+) IR and incubated for an additional 1 h. The levels of DNA-PK_{CS} and DNA-PK_{CS} phosphorylated at S2056 were examined by immunoblotting.

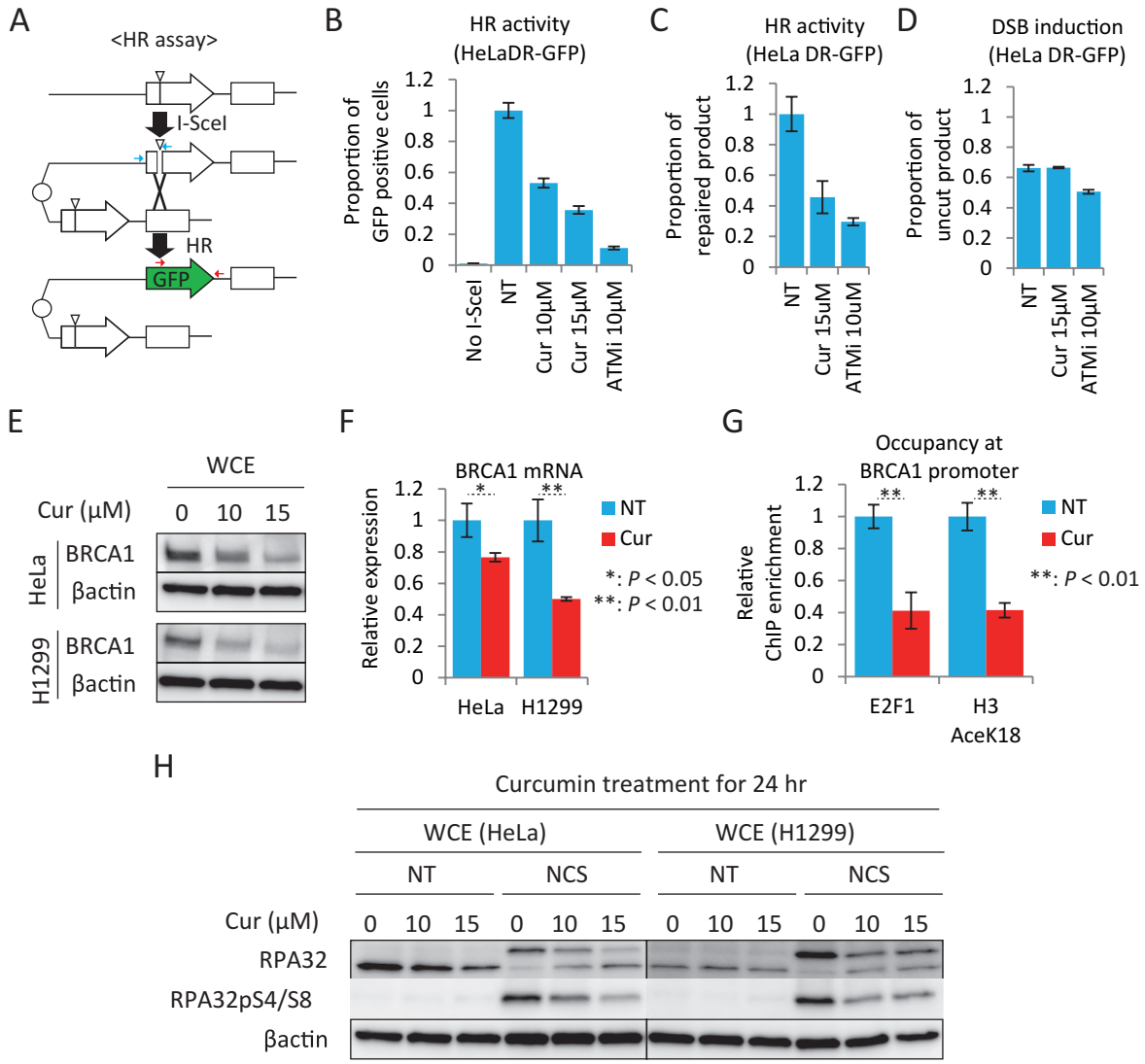

Fig. 2. Curcumin suppresses the transcriptional expression of BRCA1. (**A**) HR assay design. I-*Sce*I sites are indicated by large white arrows. The locations of the primers for quantitative PCR, used to monitor the introduction of DSBs by I-*Sce*I (uncut DNA) and subsequent repair (repaired DNA), are indicated by small blue and red arrows, respectively. (**B**) Suppression of *I-Sce*I-induced HR by treatment with curcumin. HeLa DR-GFP cells, after treatment with or without curcumin or ATM inhibitor, were either transfected with an *I-Sce*I expression plasmid or mock-transfected (No I-*Sce*I). Forty-eight hours after transfection, cells were harvested and assayed for GFP expression by flow cytometry. The proportion of GFP-positive cells detected after inhibitor treatment is expressed as a ratio relative to the proportion detected in the non-treated (NT) sample. Data represent the means ± SD of triplicate experiments. (**C** and **D**) Assessment of DSB generation and repair. (C) Proportion of repaired product 48 h after transfection with the I-*Sce*I expression plasmid. The proportion of repaired product detected after inhibitor treatment is expressed as a ratio relative to the proportion detected in the NT sample. (D) Proportion of uncut product at the I-*Sce*I site 24 h after transfection with the I-*Sce*I expression plasmid. The proportion of uncut product detected after inhibitor treatment is expressed as a ratio relative to the amount of uncut product present before transfection with I-*Sce*I expression plasmid. Data represent the means ± SD of triplicate experiments. (**E**) Downregulation of BRCA1 in curcumin-treated cells. HeLa and H1299 cells were treated for 24 h and harvested, and whole-cell extracts were subjected to immunoblotting. (**F**) Reduction of *BRCA1* transcript in curcumin-treated cells. HeLa and H1299 cells were treated for 24 h. The cells were harvested and subjected to quantitative real-time PCR for the detection of *BRCA1* mRNA. Expression levels were normalized against the levels of GAPDH mRNA. Data represent the means ± SD. Each experiment was performed in triplicate, and the results are shown as the means ± SD. Asterisks indicate statistically significant differences between curcumin-treated and untreated cells, as determined by Student's *t*-test (*$P < 0.05$; **$P < 0.01$) (F and **G**). (G) Impaired histone acetylation and changes in E2F1 binding at the *BRCA1* promoter region caused by treatment with curcumin. H1299 cells pretreated with or without curcumin for 24 h were subjected to ChIP assays. DNA immunoprecipitated with antibodies against acetylated H3 K18 (H3 AceK18) or E2F1 was subjected to quantitative PCR to detect the promoter region of *BRCA1*. The relative ChIP enrichment was calculated by dividing the ChIP enrichment at the *BRCA1* promoter in the curcumin-treated sample by the ChIP enrichment at the *BRCA1* promoter in the non-treated sample. Data represent the means ± SD of triplicate experiments. (**H**) Impact of long-term curcumin treatment on NCS-induced phosphorylation of RPA32. HeLa and H1299 cells pretreated with curcumin (0, 10 or 15 μM) for 24 h (long term) were treated with 0 (NT) or 500 μg/ml NCS and then subjected to immunoblotting 2 h later. The levels of RPA32 and RPA32 phosphorylated at Ser4/Ser8 were analyzed using the indicated antibodies.

whereas CHK2 phosphorylation, reflecting ATM-CHK2 signaling, was not. A similar result was observed upon siRNA-mediated knockdown of ATR but not upon inhibition of ATM (Figure 4B and C). Impairment of CHK1 phosphorylation by curcumin was also observed following CPT or NCS treatment of HeLa, H1299, and HT1080 cells (Figure 4D). These results led us to hypothesize that curcumin inhibits the kinase activity of ATR.

To test this idea, we performed an *in vitro* ATR kinase assay using an ATR-ATRIP complex constituted from recombinant proteins (47). Phosphorylation of the substrate protein RAD17 was suppressed by curcumin in a dose-dependent manner, with an IC_{50} of 493 nM (Figure 4E; Supplementary Figure S6, available at *Carcinogenesis* Online). To confirm further the effects of ATR inhibition by curcumin *in vivo*, we monitored DNA damage-induced

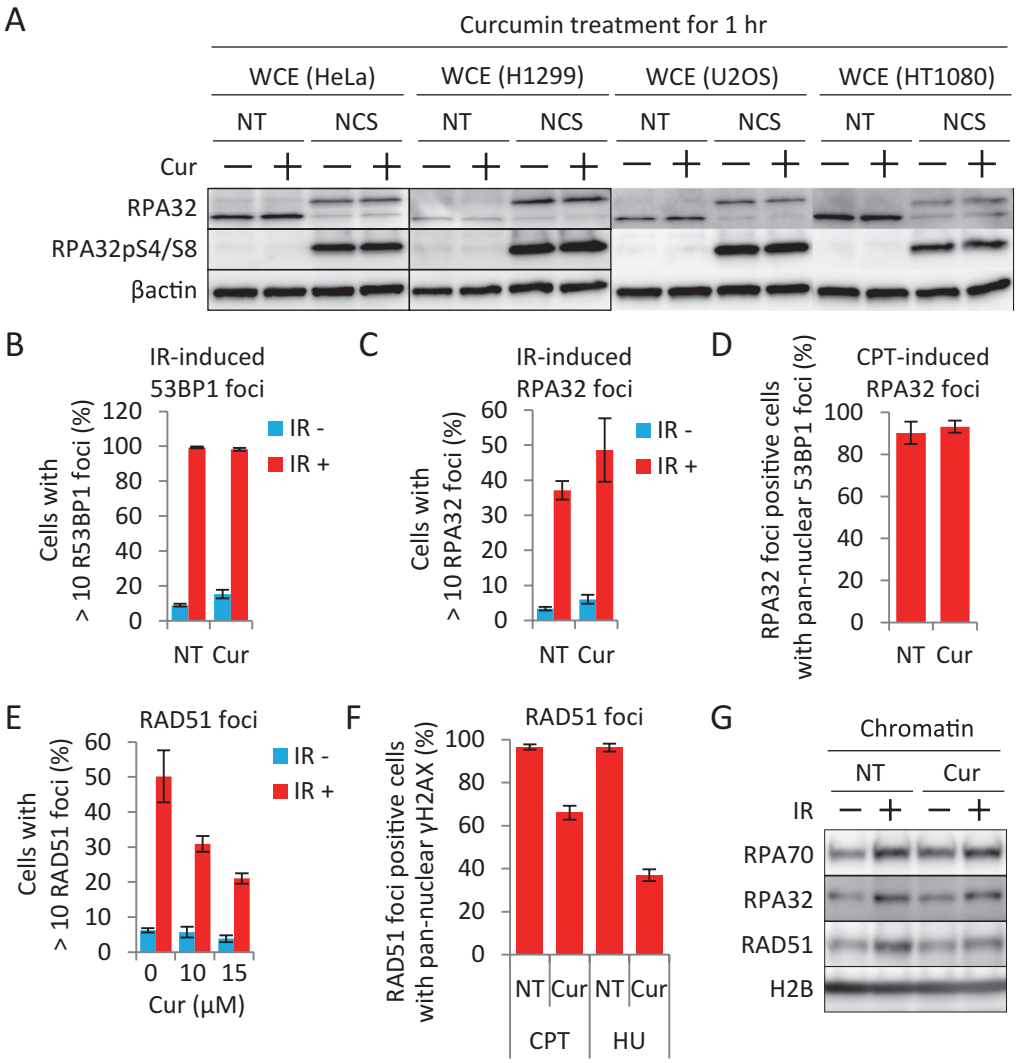

Fig. 3. Curcumin suppresses HR at the step of RAD51 assembly. (**A**) Impact of short-term curcumin treatment on NCS-induced phosphorylation of RPA32. HeLa, H1299, U2OS and HT1080 cells pretreated with curcumin (0 [–] or 15 μM [+]) for 1 h were treated with 0 (NT) or 500 μg/ml NCS and then subjected to immunoblotting 2 h later. The levels of RPA32 and RPA32 phosphorylated at Ser4/Ser8 were determined using the indicated antibodies. (**B** and **C**) Impact of curcumin on IR-induced formation of RPA32 and 53BP1 foci. HeLa cells were treated either with control (NT) or 15 μM curcumin (Cur). One hour after treatment, the cells were treated with 0 (IR–) or 10 Gy IR (IR+) and incubated for 4 h before being fixed and processed for (C) RPA32 and (**D**) 53BP1 immunofluorescence analysis. Representative immunofluorescence images are shown in Supplementary Figure S5A, available at *Carcinogenesis* Online. Foci-positive cells were defined as cells with >10 foci. The experiments were repeated at least twice, and representative results are shown. The percentage of foci-positive cells was determined from >100 cells per sample; each of these experiments was performed in triplicate, and the results are shown as the means ± SD (**B**–**F**). (**D**) Impact of CPT-induced formation of RPA32 foci by curcumin. HeLa cells were treated either with control (NT) or 15 μM curcumin (Cur). One hour after treatment, the cells were treated with 1 μM CPT for 3 h before being fixed and processed for RPA32 and 53BP1 immunofluorescence analysis. Representative immunofluorescence images are shown in Supplementary Figure S5B, available at *Carcinogenesis* Online. The percentages of RPA32 foci-positive cells containing pan-53BP1 foci are shown in the graph on the right. (**E**) Suppression of IR-induced formation of RAD51 foci by curcumin. HeLa cells were treated with control (NT) or 10 or 15 μM curcumin. One hour after treatment, cells were treated with 0 (IR–) or 10 Gy IR (IR+) and incubated for 4 h before being fixed and processed for RAD51 and γH2AX immunofluorescence analysis. Representative immunofluorescence images are shown in Supplementary Figure S5D, available at *Carcinogenesis* Online. Foci-positive cells were defined as cells with >10 RAD51 foci. (F) Suppression of CPT- and HU-induced formation of RAD51 foci by curcumin. HeLa cells were treated with control (NT) or 15 μM curcumin (Cur). One hour after treatment, cells were treated with 1 μM CPT or 5 mM HU for 3 h before being fixed and processed for RAD51 and γH2AX immunofluorescence analysis. Representative images are shown in Supplementary Figure S5E, available at *Carcinogenesis* Online. Percentages of RAD51-foci-positive cells with pan-nuclear gamma-H2AX (indicating cells damaged in S phase) are shown. (**G**) Decreased DNA damage-induced chromatin binding of RPA and RAD51 proteins upon treatment with curcumin. HeLa cells pretreated with curcumin for 1 h were treated with 0 Gy (–) or 10 Gy (+) IR and harvested 3 h after irradiation. Chromatin-enriched fractions were subjected to immunoblot analysis.

autophosphorylation of the Thr1989 residue of ATR, which represents the active state of the ATR protein (47). Consistent with the results of the *in vitro* kinase assay, phosphorylation of Thr1989 in response to IR, HU and CPT was suppressed by curcumin *in vivo* (Figure 4F). HU induces ATR-dependent phosphorylation of serine residues 4 and 8 within the RPA protein (55–57). Treatment with curcumin reduced the proportion of HU-treated cells with phosphorylated RPA32 foci among cells that contained pan-nuclear RPA32 foci (Figure 4G; Supplementary Figure S7, available at *Carcinogenesis* Online). Consistent with this, curcumin treatment also reduced the fraction of phosphorylated RPA32 induced by HU (Figure 4H). These results demonstrate that, as we hypothesized, curcumin suppresses HR by inhibiting the kinase activity of ATR.

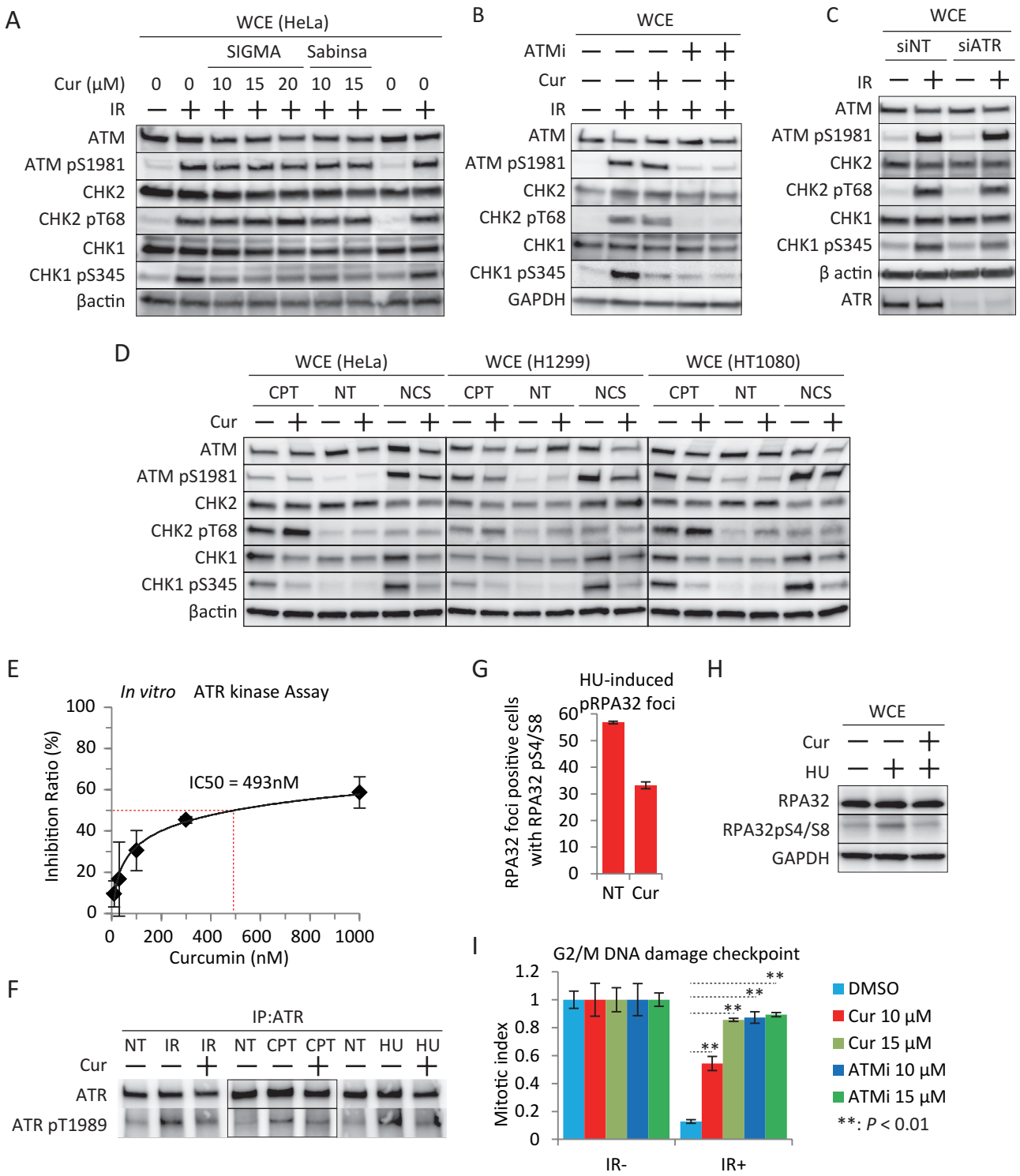

Fig. 4. Curcumin suppresses activation of ATR and induction of G_2/M DNA damage checkpoint. (**A**) Suppression of IR-induced CHK1 activation by curcumin. HeLa cells pretreated with dimethyl sulfoxide (DMSO, 0 μM) or curcumin from two different suppliers (Sigma: 10, 15 or 20 μM; Sabinsa: 10 or 15 μM) for 1 h were treated with 0 Gy (–) or 10 Gy (+) IR and subjected to immunoblotting 1 h later. (**B**) Suppression of IR-induced CHK1 activation by curcumin or an ATM inhibitor. HeLa cells pretreated with DMSO, 10 μM curcumin and/or 10 μM ATM inhibitor (KU55933) for 1 h were treated with 10 Gy IR and subjected to immunoblotting 1 h later. (**C**) Suppression of IR-induced CHK1 activation by ATR depletion. HeLa cells were treated with control (siNT) or ATR (siATR) siRNA for 48 h. The cells were then treated with 0 (–) or 10 Gy IR (+) and subjected to immunoblotting 1 h later. (**D**) Suppression of CPT- and NCS-induced CHK1 activation by curcumin. HeLa cells pretreated with DMSO (–) or 15 μM curcumin (+) for 1 h were treated with 1 μM CPT, 500 μg/ml NCS or no additional drug (NT), and subjected to immunoblotting 2 h later. (**E**) Suppression of *in vitro* ATR kinase activity by curcumin. HEK293E cells were transfected with Flag-ATR- and His-ATRIP-expressing plasmids, and the ATR-ATRIP complex was purified. The kinase reactions were performed using purified ATR-ATRIP complex, GST-Rad17 and adenosine triphosphate in the presence or absence of curcumin. The concentration of curcumin that achieved 50% inhibition of the enzyme (IC_{50}) was derived from log approximation plots. Enzyme activity was plotted against the concentration of curcumin. Data represent the means ± SD of triplicated experiments. (**F**) Suppression of damage-induced ATR activation by curcumin. HeLa cells pretreated with DMSO (–) or 15 μM curcumin (+) for 1 h were treated with 10 Gy IR, 1 μM CPT, 5 mM HU or no additional treatment (NT), and subjected to immunoprecipitation with anti-ATR antibody 3 h later. The levels of precipitated

ATR-CHK1 signaling regulates not only HR but also the DNA damage checkpoint (31). Therefore, we next investigated whether curcumin also abrogates the DNA damage checkpoint. IR treatment reduced the proportion of cells containing phosphorylated histone H3 (Ser10), a mitotic marker, indicating that irradiated cells underwent cell cycle arrest at G_2 via activation of the G_2/M DNA damage checkpoint. This reduction in H3-Ser10 phosphorylation was prevented by curcumin treatment (Figure 4I). Thus, by inhibiting ATR, curcumin suppresses not only HR but also the DNA damage checkpoint.

Curcumin inhibits the activity of IKKβ, an activator of the NF-κB pathway, which regulates several cellular responses against DNA damage. Therefore, we investigated whether the inhibition of this pathway might also contribute to the suppression of HR and the DNA damage checkpoint. Inhibition of IKKβ by treatment with a specific inhibitor at the IC_{50} did not affect activation of the G_2/M DNA damage checkpoint or IR-induced formation of RAD51 foci (Supplementary Figure S1F and G, available at *Carcinogenesis* Online). However, this inhibitor significantly suppressed HR activity in the DR-GFP assay (Supplementary Figure S1H, available at *Carcinogenesis* Online), suggesting that the IKK-mediated NF-κB pathway enhances steps of HR downstream of RAD51. These results further support the idea that curcumin inhibits CBP/p300-mediated histone acetylation at DSB sites and the *BRCA1* promoter region, as well as ATR-dependent CHK1 activation, resulting in suppression of HR and the DNA damage checkpoint response.

Curcumin sensitizes cancer cells to PARP inhibitors

Deficiencies in HR and the DNA damage checkpoint make cancer cells sensitive to PARP inhibitors (58). Therefore, we predicted that curcumin might act as a sensitizer for cancer cell death induced by PARP inhibition. Indeed, treatment with curcumin sensitized HeLa cells to a PARP inhibitor, olaparib, which has been extensively tested in clinical trials (58) (Figure 5A). The sensitization was also observed for another PARP inhibitor, 4-amino-1,8-naphthalimide (Figure 5A). We also observed sensitization to one of these PARP inhibitors in three other cancer cell lines (Figure 5B). HeLa cells were also sensitized to the DSB-inducing agents CPT and HU (Figure 5C). These results strongly suggest that by suppressing responses against DSBs, curcumin can sensitize a variety of cancer cells with intact BRCA1/2-mediated DDRs to PARP inhibitors.

We next investigated the mechanism underlying curcumin-induced sensitization to PARP inhibitors. Curcumin suppressed PARP inhibitor-induced CHK1 activation without affecting the activation of the ATM-CHK2 pathway (Figure 5D). Olaparib increases the proportion of γH2AX-positive cells in a concentration-dependent manner; these increases were more evident following combined treatment with curcumin (Figure 5E; Supplementary Figure S8A, available at *Carcinogenesis* Online). Cell cycle analysis revealed that the proportion of cells in the G_2/M phase was higher in cells co-treated with olaparib and curcumin than in cells treated with either drug alone (Supplementary Figure S8B, available at *Carcinogenesis* Online). In addition, combination treatment also increased the proportions of sub-G_1 and >4N cells, which represent cells undergoing death due to apoptosis and mitotic catastrophe, respectively (Supplementary Figure S8B, available at *Carcinogenesis* Online). Consistent with this, flow cytometry analysis of Annexin V/PI-stained cells confirmed that combined treatment with olaparib and curcumin increased the proportion of apoptotic cells (Figure 5F; Supplementary Figure S8C, available at *Carcinogenesis* Online). In addition, the proportion of morphologically abnormal micronucleated cells, representing cells undergoing mitotic catastrophe, also increased upon combined treatment (Figure 5G; Supplementary Figure S8D, available at *Carcinogenesis* Online). These results indicate that curcumin abrogates both DNA repair and the DNA damage checkpoint in response to DSBs generated by PARP inhibition, resulting in accumulation of DSBs and cell death via apoptosis and mitotic catastrophe.

Discussion

The results of this study demonstrate that curcumin suppresses three major DDRs against genotoxic events mediated by PARP inhibition: NHEJ, HR and the G_2/M DNA damage checkpoint (Figure 6). This suppression results from the inhibition of CBP/p300 HATs and ATR kinase. The impact of curcumin on NHEJ is mediated by the suppression of histone acetylation at DSB sites, which prevents accumulation of NHEJ proteins, e.g. KU70/KU80, that are responsible for DNA synapsis. This is consistent with the outcome of CBP/p300 depletion (22). In addition, it is also possible that NHEJ suppression by curcumin is caused by inhibition of AKT1 kinase, involved in the activation of DNA-PK_{CS} along with KU70/KU80 (43,45), or by inhibition of IKKβ, an activator of NF-κB, which is involved in DDRs in a variety of ways (44). However, curcumin suppressed the IR-induced phosphorylation of DNA-PK_{CS}, but not AKT, suggesting that NHEJ suppression by curcumin is mainly due to inhibition of KU70/KU80 accumulation, which is essential for DNA-PK_{CS} activation. In addition, inhibition of IKKβ by a specific inhibitor, BMS-345541, did not suppress NHEJ activity. These results indicate that the suppression of the activities of the histone acetyltransferases CBP and p300 is a major mechanism of NHEJ suppression by curcumin.

As in the case of NHEJ, the impact of curcumin on HR was also mediated by the suppression of histone acetylation at DSB sites. In addition, suppression of histone acetylation at the promoter region of the *BRCA1* gene was also likely to be responsible: BRCA1 contributes to DNA end resection at DSBs by forming the BRCA1-CtIP-MRN complex, which promotes binding of RPA and RAD51 to ssDNA, followed by formation of RAD51/RPA foci that undergo HR. These phenomena were suppressed by curcumin treatment. As noted above, we recently showed that the knockdown of CBP/p300 leads to the transcriptional repression of the *BRCA1* gene, associated with decreases in both histone acetylation and accumulation of E2F1 transcription factor at the promoter region. Therefore, suppression of *BRCA1* expression by curcumin is likely to be caused by inhibition of CBP/p300 HAT activities. In this study, inhibition of IKKβ by a specific inhibitor, BMS-345541, did not suppress NHEJ or the DNA damage checkpoint, but it did suppress HR in the DR-GFP assay without affecting RAD51 assembly. Therefore, IKKβ inhibition by curcumin might represent an additional mechanism of HR suppression, i.e. via inhibition of the steps of HR downstream of RAD51 assembly. Thus, inhibition of CBP/p300-mediated histone acetylation at DSB sites and the *BRCA1* promoter region is a major mechanism for the suppression of HR by curcumin.

←
ATR and ATR-pT1989 were analyzed using the indicated antibodies. (**G**) Suppression of HU-induced formation of phosphorylated RPA32 foci by curcumin. HeLa cells were treated with DMSO (NT) or 15 μM curcumin (Cur). One hour after treatment, the cells were treated with 5 mM HU for 3 h. Percentages are shown of cells containing foci of pan-nuclear RPA32, which were positive for RPA phosphorylated at Ser4/Ser8. Data represent the mean ± SD. The percentage of foci-positive cells was determined from >100 cells per sample, and each experiment was performed in triplicate. (**H**) Reduction in HU-induced phosphorylated RPA32 protein levels after treatment with curcumin. HeLa cells pretreated with DMSO (–) or 15 μM curcumin (+) for 1 h were treated with 0 (–) or 5 mM HU (+) and then subjected to immunoblotting 3 h later. The levels of RPA32 and RPA32 phosphorylated at Ser4/Ser8 were analyzed using the indicated antibodies. (**I**) Suppression of the G_2/M DNA damage checkpoint by curcumin. HeLa cells were treated with DMSO, curcumin (Cur 10 or 15 μM) or the ATM inhibitor KU55933 (ATMi 10 or 15 μM) for 1 h. The cells were then irradiated with 3 Gy (IR) or not irradiated (NT) and then 1 h later were stained with PI and antibodies against phospho-histone H3. The percentage of mitotic cells (mitotic index) was determined by flow cytometry. Data represent the means ± SD. Each experiment was performed in triplicate. Asterisks indicate a significant difference between curcumin-treated and untreated cells, as determined by Student's *t*-test (**$P < 0.01$).

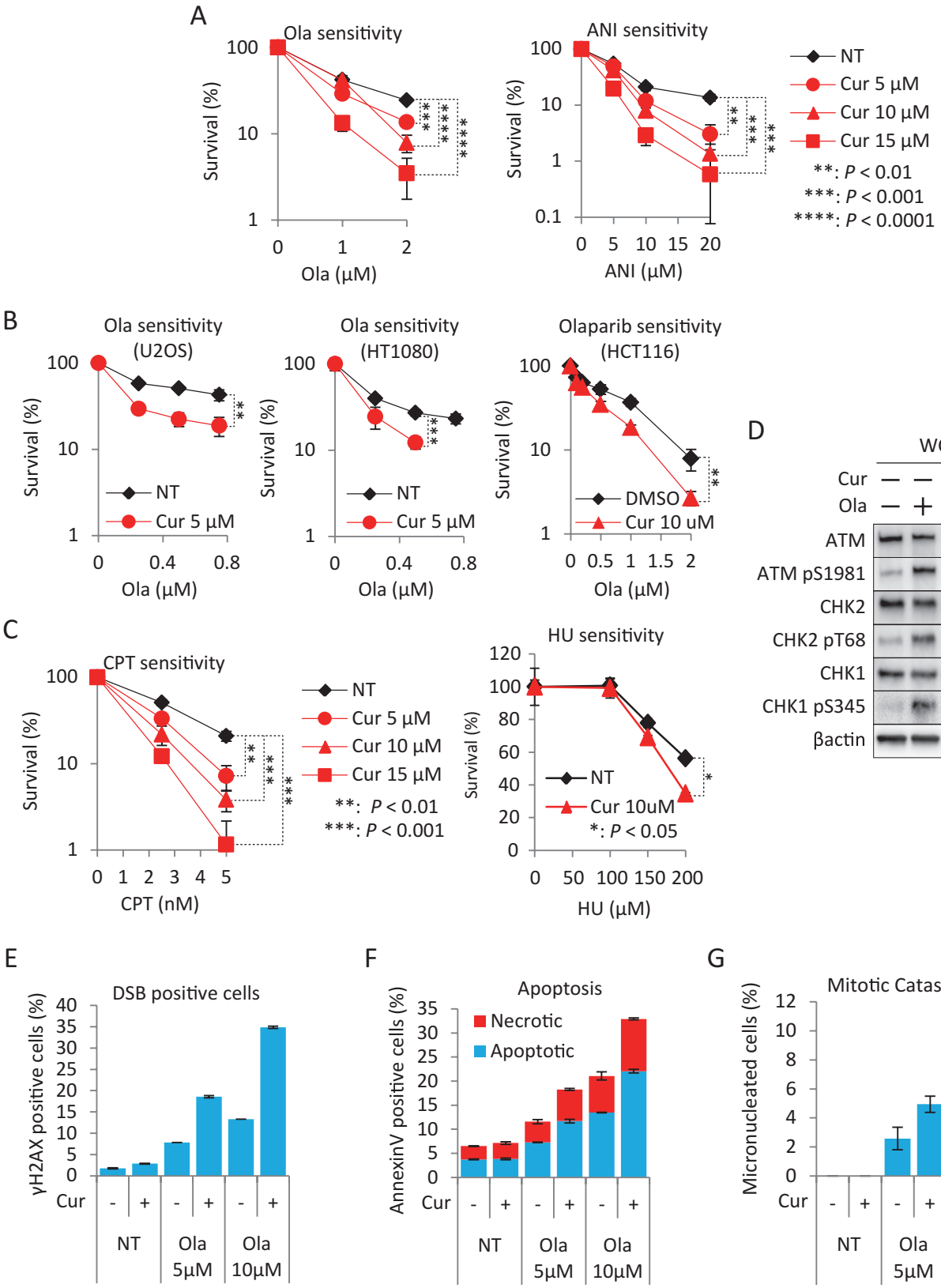

Fig. 5. Curcumin sensitizes cancer cells to PARP inhibitors by induction of DSB accumulation, apoptosis and mitotic catastrophe. (**A**) Colony formation of HeLa cells treated with olaparib (left) or 4-amino-1,8-naphthalimide (right) and 0, 5, 10 or 15 μM curcumin. Data represent the means ± SD. Each experiment was performed in triplicate. Asterisks indicate a significant difference between curcumin-treated and untreated cells, as determined by Student's *t*-test (*$P < 0.05$, **$P < 0.01$; ***$P < 0.001$; ****$P < 0.0001$) (**A–C**). (B) Curcumin sensitizes various cancer cells to PARP inhibitors. Colony formation of U2OS, HT1080 and HCT116 cells treated with varying concentrations of olaparib (Ola) and with 0 (NT), 5 or 10 μM curcumin (Cur). Survival is expressed as the percentage ± standard deviation of colonies formed relative to the corresponding samples treated with 0 μM olaparib. (C) Curcumin sensitizes cancer cells to CPT and HU. Colony formation of HeLa cells treated with CPT (left) or HU (right) with 0 (NT) or 10 μM curcumin (Cur). Survival is expressed as the percentage ± standard deviation of colonies formed

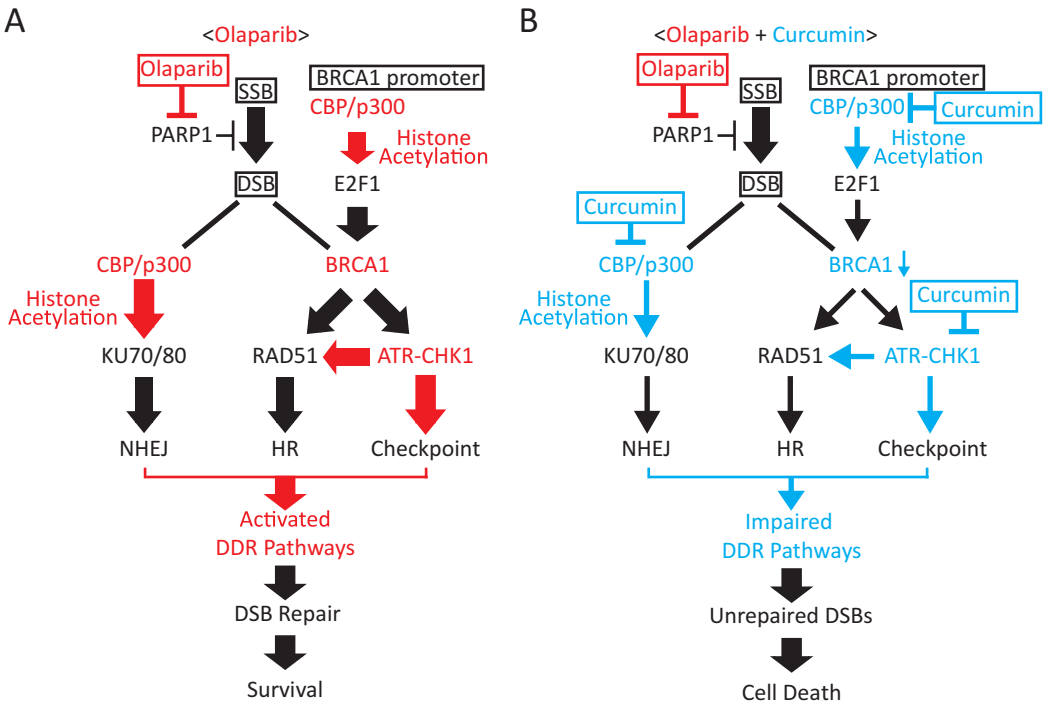

Fig. 6. Model: How curcumin inhibits three major DNA damage responses. (**A**) Activation of DDRs by the PARP inhibitor olaparib. (**B**) Suppression of DDRs activated by olaparib in combination with curcumin. The PARP inhibitor suppresses repair of DNA SSBs. Unrepaired SSBs are converted to DNA DSBs by collapse of stalled replication forks during DNA replication. In the NHEJ pathway, curcumin inhibits CBP and p300, reducing histone acetylation at DSB sites, causing KU70/80 to fail to accumulate at DSBs and ultimately leading to suppression of NHEJ. Curcumin suppresses HR through reduction of CBP/p300-mediated histone acetylation at DSBs and at the *BRCA1* promoter, resulting in reduced BRCA1 expression. Curcumin also inhibits ATR kinase, leading to suppression of CHK1-dependent RAD51 activation and the DNA damage checkpoint pathway. Curcumin-mediated suppression of DSB repair pathways and the DNA damage checkpoint results in the accumulation of DSBs and induction of cell death by apoptosis and mitotic catastrophe.

ATR-CHK1 signaling is critical to both HR and the DNA damage checkpoint and is essential for survival following treatment with a PARP inhibitor (31,59). Our results here reveal a novel activity of curcumin, i.e. inhibition of the kinase activity of ATR, which regulates HR and the DNA damage checkpoint. Curcumin treatment suppressed ATR-CHK1 but not ATM-CHK2 signaling in response to treatments with PARP inhibitors and other DNA-damaging agents such as CPT and NCS. Previously, in contrast to our results, another group reported that curcumin treatment activates CHK1 (60,61). In those studies, the authors observed that CHK1 and ATM, but neither CHK2 nor ATR, were phosphorylated following treatment with curcumin for 24–48 h and that CHK1 phosphorylation was dependent on ATM activity. By contrast, under our experimental conditions, CHK1 phosphorylation and γH2AX were not induced even after a 24 h treatment, and NCS-induced CHK1 phosphorylation was also suppressed by a 24 h curcumin treatment (Supplementary Figure S9, available at *Carcinogenesis* Online). Therefore, we speculate that curcumin does indeed inhibit ATR-dependent CHK1 phosphorylation, but that long-term exposure of curcumin causes ATM activation by abrogating multiple DDR pathways following ATM-dependent CHK1 phosphorylation.

PARP inhibitors are promising drugs for the treatment of BRCA1/BRCA2-associated cancers; however, to utilize PARP inhibitors in clinical settings, efficient therapeutic strategies are required, particularly for cancers in which BRCA1 and BRCA2 mutations rarely occur (62). Sensitization to PARP inhibitors is predicted to occur as a result of inhibition of DDRs including NHEJ, HR and the DNA damage checkpoint (37). The results of this study indicate that curcumin suppresses all three of these DDRs by inhibition of CBP/p300 HATs and ATR kinase and thereby confers sensitivity to PARP inhibitors on cancer cells that retain BRCA1/2-mediated DDRs.

Other effects of curcumin are also potentially related to sensitization. PARP1 is an activator of E2F1 and CBP/p300 (63), and transcription of the gene encoding the ATR activator Claspin, as well as expression of CHK1 and RAD51, is positively regulated by E2F1 (64,65). Therefore, curcumin treatment might lead to repression of not only *BRCA1* but also other E2F1 target genes involved in DDR pathways. Furthermore, in light of our finding that curcumin enhances the accumulation of DSBs, apoptosis and mitotic catastrophe induced by PARP inhibitors, curcumin-mediated inhibition of the antiapoptotic

←
relative to the corresponding samples not treated with HU or CPT (i.e. 0 μM). (**D**) Suppression of olaparib-induced CHK1 activation by curcumin. HeLa cells were pretreated with DMSO or 15 μM curcumin for 1 h; treated with DMSO, 10 μM olaparib, 15 μM curcumin or a combination of curcumin and olaparib and then subjected to immunoblotting 6 h later. (**E**) Accumulation of olaparib-induced DSBs was increased by curcumin treatment. HeLa cells were treated with DMSO (NT) or olaparib (5 or 10 μM) in the presence (+) or absence (−) of 10 μM curcumin for 72 h, followed by staining with antibodies against phospho-histone H2AX (Ser139; γH2AX) and with PI. The percentage of γH2AX-positive cells was determined by flow cytometry. Data represent the means ± SD of triplicate experiments. (**F**) Apoptosis in cells treated with curcumin and olaparib. HeLa cells were treated with DMSO (NT) or olaparib (5 or 10 μM) in the presence (+) or absence (−) of 10 μM curcumin for 96 h and then stained with Annexin V (conjugated to fluorescein isothiocyanate) and PI. The percentage of Annexin V-positive cells (early and late apoptotic cells) is represented as the mean ± SD of triplicate experiments. (**G**) Mitotic catastrophe in curcumin/olaparib-treated cells. HeLa cells were treated with DMSO (NT) or olaparib (5 μM or 10 μM) in the presence (+) or absence (−) of 10 μM curcumin for 96 h before being fixed and processed for nuclear staining with 4′,6-diamidino-2-phenylindole or for α-tubulin/γH2AX immunofluorescence analysis. Representative images of micronucleated cells are shown in Supplementary Figure S15D, available at *Carcinogenesis* Online. The percentages of micronucleated cells are represented as the means ± SD of triplicate experiments.

functions of both the NF-κB pathway and the ATR-CHK1 cell-cycle checkpoint pathway might also play significant roles. These points should be further investigated to comprehensively elucidate the effects of curcumin on DDRs.

Recently, specific inhibitors against ATR kinase have been identified, and their utility in cancer therapy will be tested in future studies (66,67); in particular, their safety and tolerability in humans are unknown and must be investigated. On the other hand, curcumin has been examined in several clinical studies for its anticancer and chemosensitizing activities (39), and its low toxicity in humans has been amply demonstrated (6–8,38). Considering that it suppresses not only ATR but also CBP/p300 HATs, which positively regulates two major DSB repair pathways, and also possibly enhances apoptosis and mitotic catastrophe, curcumin is a strong candidate for a drug that could be used to increase the efficacy of PARP inhibitor-based therapies.

In conclusion, this study demonstrates that curcumin suppresses multiple DDRs, including NHEJ, HR and the G_2/M DNA damage checkpoint, by inhibiting CBP/p300 HATs and ATR kinase. These DDRs are critical for recovery from DSBs generated by the actions of PARP inhibitors. NHEJ and HR are the two major DSB repair pathways involving BRCA1/2. ATR-CHK1 signaling is critical for the induction of cell death via apoptosis and mitotic catastrophe in response to persistent DSBs. Consistent with this, curcumin enhanced the sensitivity to PARP inhibitors of DDR-proficient cancer cells by inducing both apoptosis and mitotic catastrophe, indicating its potential utility as a sensitizer for PARP inhibitor-based cancer therapy. Notably, higher concentrations of curcumin led to greater sensitization to DNA-damaging agents and greater suppression of DDRs. Therefore, delivery of curcumin to tumor cells at high concentrations might be necessary to achieve optimal sensitization. Ongoing studies using animal models in our laboratory will determine the effects of sensitization to PARP inhibitors *in vivo*.

Supplementary material

Supplementary Materials and methods and Figures 1–9 can be found at http://carcin.oxfordjournals.org/

Funding

Grant-in-Aid from the Ministry of Education, Culture, Sports, Science, and Technology of Japan for Scientific Research on Innovative Areas (22131006); Grant-in-Aid from the Japan Society for the Promotion of Science for Young Scientists (B) KAKENHI (23701110); Management Expenses Grants from the Government to the National Cancer Center; Cooperative Research Project Program of the Institute of Development, Aging, and Cancer of Tohoku University.

Acknowledgements

We greatly appreciate the support from all members of the Kohno laboratory.

Conflict of Interest Statement: None declared.

References

1. Narod,S.A. (2010) BRCA mutations in the management of breast cancer: the state of the art. *Nat. Rev. Clin. Oncol.*, **7**, 702–707.
2. Helleday,T. *et al.* (2005) Poly(ADP-ribose) polymerase (PARP-1) in homologous recombination and as a target for cancer therapy. *Cell Cycle*, **4**, 1176–1178.
3. Farmer,H. *et al.* (2005) Targeting the DNA repair defect in BRCA mutant cells as a therapeutic strategy. *Nature*, **434**, 917–921.
4. Bryant,H.E. *et al.* (2005) Specific killing of BRCA2-deficient tumours with inhibitors of poly(ADP-ribose) polymerase. *Nature*, **434**, 913–917.
5. Bryant,H.E. *et al.* (2006) Inhibition of poly (ADP-ribose) polymerase activates ATM which is required for subsequent homologous recombination repair. *Nucleic Acids Res.*, **34**, 1685–1691.
6. Tutt,A. *et al.* (2010) Oral poly(ADP-ribose) polymerase inhibitor olaparib in patients with BRCA1 or BRCA2 mutations and advanced breast cancer: a proof-of-concept trial. *Lancet*, **376**, 235–244.
7. Fong,P.C. *et al.* (2009) Inhibition of poly(ADP-ribose) polymerase in tumors from BRCA mutation carriers. *N. Engl. J. Med.*, **361**, 123–134.
8. Audeh,M.W. *et al.* (2010) Oral poly(ADP-ribose) polymerase inhibitor olaparib in patients with BRCA1 or BRCA2 mutations and recurrent ovarian cancer: a proof-of-concept trial. *Lancet*, **376**, 245–251.
9. Ledermann,J. *et al.* (2012) Olaparib maintenance therapy in platinum-sensitive relapsed ovarian cancer. *N. Engl. J. Med.*, **366**, 1382–1392.
10. Kaye,S.B. *et al.* (2012) Phase II, open-label, randomized, multicenter study comparing the efficacy and safety of olaparib, a poly (ADP-ribose) polymerase inhibitor, and pegylated liposomal doxorubicin in patients with BRCA1 or BRCA2 mutations and recurrent ovarian cancer. *J. Clin. Oncol.*, **30**, 372–379.
11. Mahajan,K.N. *et al.* (2002) Association of DNA polymerase mu (pol mu) with Ku and ligase IV: role for pol mu in end-joining double-strand break repair. *Mol. Cell. Biol.*, **22**, 5194–5202.
12. Lieber,M.R. *et al.* (2003) Mechanism and regulation of human non-homologous DNA end-joining. *Nat. Rev. Mol. Cell Biol.*, **4**, 712–720.
13. Valerie,K. *et al.* (2003) Regulation and mechanisms of mammalian double-strand break repair. *Oncogene*, **22**, 5792–5812.
14. Lieber,M.R. (2010) The mechanism of double-strand DNA break repair by the nonhomologous DNA end-joining pathway. *Annu. Rev. Biochem.*, **79**, 181–211.
15. Golding,S.E. *et al.* (2009) Pro-survival AKT and ERK signaling from EGFR and mutant EGFRvIII enhances DNA double-strand break repair in human glioma cells. *Cancer Biol. Ther.*, **8**, 730–738.
16. Ma,Y. *et al.* (2004) A biochemically defined system for mammalian nonhomologous DNA end joining. *Mol. Cell*, **16**, 701–713.
17. van Gent,D.C. *et al.* (2007) Non-homologous end-joining, a sticky affair. *Oncogene*, **26**, 7731–7740.
18. Lieber,M.R. (2008) The mechanism of human nonhomologous DNA end joining. *J. Biol. Chem.*, **283**, 1–5.
19. Ma,Y. *et al.* (2002) Hairpin opening and overhang processing by an Artemis/DNA-dependent protein kinase complex in nonhomologous end joining and V(D)J recombination. *Cell*, **108**, 781–794.
20. Ogiwara,H. *et al.* (2011) Essential factors for incompatible DNA end joining at chromosomal DNA double strand breaks *in vivo*. *PLoS One*, **6**, e28756.
21. Mukherjee,B. *et al.* (2012) The dual PI3K/mTOR inhibitor NVP-BEZ235 is a potent inhibitor of ATM- and DNA-PKCs-mediated DNA damage responses. *Neoplasia*, **14**, 34–43.
22. Ogiwara,H. *et al.* (2011) Histone acetylation by CBP and p300 at double-strand break sites facilitates SWI/SNF chromatin remodeling and the recruitment of non-homologous end joining factors. *Oncogene*, **30**, 2135–2146.
23. Flygare,J. *et al.* (1996) Expression of the human RAD51 gene during the cell cycle in primary human peripheral blood lymphocytes. *Biochim. Biophys. Acta*, **1312**, 231–236.
24. Ciccia,A. *et al.* (2010) The DNA damage response: making it safe to play with knives. *Mol. Cell*, **40**, 179–204.
25. Chen,L. *et al.* (2008) Cell cycle-dependent complex formation of BRCA1.CtIP.MRN is important for DNA double-strand break repair. *J. Biol. Chem.*, **283**, 7713–7720.
26. Sartori,A.A. *et al.* (2007) Human CtIP promotes DNA end resection. *Nature*, **450**, 509–514.
27. Wold,M.S. (1997) Replication protein A: a heterotrimeric, single-stranded DNA-binding protein required for eukaryotic DNA metabolism. *Annu. Rev. Biochem.*, **66**, 61–92.
28. West,S.C. (2003) Molecular views of recombination proteins and their control. *Nat. Rev. Mol. Cell Biol.*, **4**, 435–445.
29. Sørensen,C.S. *et al.* (2005) The cell-cycle checkpoint kinase Chk1 is required for mammalian homologous recombination repair. *Nat. Cell Biol.*, **7**, 195–201.
30. Zou,L. *et al.* (2003) Sensing DNA damage through ATRIP recognition of RPA-ssDNA complexes. *Science*, **300**, 1542–1548.
31. Cimprich,K.A. *et al.* (2008) ATR: an essential regulator of genome integrity. *Nat. Rev. Mol. Cell Biol.*, **9**, 616–627.
32. Munck,J.M. *et al.* (2012) Chemosensitization of cancer cells by KU-0060648, a dual inhibitor of DNA-PK and PI-3K. *Mol. Cancer Ther.*, **11**, 1789–1798.

33. Huang,X. *et al.* (2005) DNA damage-induced mitotic catastrophe is mediated by the Chk1-dependent mitotic exit DNA damage checkpoint. *Proc. Natl Acad. Sci. USA*, **102**, 1065–1070.
34. Castedo,M. *et al.* (2004) The cell cycle checkpoint kinase Chk2 is a negative regulator of mitotic catastrophe. *Oncogene*, **23**, 4353–4361.
35. Antoni,L. *et al.* (2007) CHK2 kinase: cancer susceptibility and cancer therapy - two sides of the same coin? *Nat. Rev. Cancer*, **7**, 925–936.
36. Cho,S.H. *et al.* (2005) Chk1 is essential for tumor cell viability following activation of the replication checkpoint. *Cell Cycle*, **4**, 131–139.
37. Plummer,R. (2010) Perspective on the pipeline of drugs being developed with modulation of DNA damage as a target. *Clin. Cancer Res*., **16**, 4527–4531.
38. Goel,A. *et al.* (2008) Curcumin as "Curecumin": from kitchen to clinic. *Biochem. Pharmacol*., **75**, 787–809.
39. Epstein,J. *et al.*. (2010) Curcumin as a therapeutic agent: the evidence from in vitro, animal and human studies. *Br. J. Nutr.*, **103**, 1545–1557.
40. Wu,L. *et al.* (2011) IKKβ regulates the repair of DNA double-strand breaks induced by ionizing radiation in MCF-7 breast cancer cells. *PLoS One*, **6**, e18447.
41. Bharti,A.C. *et al.* (2003) Curcumin (diferuloylmethane) down-regulates the constitutive activation of nuclear factor-kappa B and IkappaBalpha kinase in human multiple myeloma cells, leading to suppression of proliferation and induction of apoptosis. *Blood*, **101**, 1053–1062.
42. You,Z. *et al.* (2009) CtIP links DNA double-strand break sensing to resection. *Mol. Cell*, **36**, 954–969.
43. Toulany,M. *et al.* (2008) Targeting of AKT1 enhances radiation toxicity of human tumor cells by inhibiting DNA-PKcs-dependent DNA double-strand break repair. *Mol. Cancer Ther*., **7**, 1772–1781.
44. Surucu,B. *et al.* (2008) *In vivo* analysis of protein kinase B (PKB)/Akt regulation in DNA-PKcs-null mice reveals a role for PKB/Akt in DNA damage response and tumorigenesis. *J. Biol. Chem*., **283**, 30025–30033.
45. Bozulic,L. *et al.* (2008) PKBalpha/Akt1 acts downstream of DNA-PK in the DNA double-strand break response and promotes survival. *Mol. Cell*, **30**, 203–213.
46. Rodemann,H.P. *et al.* (2007) Radiation-induced EGFR-signaling and control of DNA-damage repair. *Int. J. Radiat. Biol*., **83**, 781–791.
47. Liu,S. *et al.* (2011) ATR autophosphorylation as a molecular switch for checkpoint activation. *Mol. Cell*, **43**, 192–202.
48. Marcu,M.G. *et al.* (2006) Curcumin is an inhibitor of p300 histone acetyltransferase. *Med. Chem*., **2**, 169–174.
49. Toledo,L.I. *et al.* (2011) Targeting ATR and Chk1 kinases for cancer treatment: a new model for new (and old) drugs. *Mol. Oncol*., **5**, 368–373.
50. Zhao,L. *et al.* (2012) Regulatory mechanisms and clinical perspectives of miRNA in tumor radiosensitivity. *Carcinogenesis*, **33**, 2220–2227.
51. Foray,N. *et al.* (2003) A subset of ATM- and ATR-dependent phosphorylation events requires the BRCA1 protein. *EMBO J*., **22**, 2860–2871.
52. Rajan,J.V. *et al.* (1996) Brca2 is coordinately regulated with Brca1 during proliferation and differentiation in mammary epithelial cells. *Proc. Natl Acad. Sci. USA*, **93**, 13078–13083.
53. Schlegel,B.P. *et al.* (2006) BRCA1 promotes induction of ssDNA by ionizing radiation. *Cancer Res*., **66**, 5181–5189.
54. Beucher,A. *et al.* (2009) ATM and Artemis promote homologous recombination of radiation-induced DNA double-strand breaks in G2. *EMBO J*., **28**, 3413–3427.
55. Block,W.D. *et al.* (2004) Phosphatidyl inositol 3-kinase-like serine/threonine protein kinases (PIKKs) are required for DNA damage-induced phosphorylation of the 32 kDa subunit of replication protein A at threonine 21. *Nucleic Acids Res*., **32**, 997–1005.
56. Peng,A. *et al.* (2005) NFBD1/Mdc1 mediates ATR-dependent DNA damage response. *Cancer Res*., **65**, 1158–1163.
57. Nuss,J.E. *et al.* (2005) DNA damage induced hyperphosphorylation of replication protein A. 1. Identification of novel sites of phosphorylation in response to DNA damage. *Biochemistry*, **44**, 8428–8437.
58. Plummer,R. (2011) Poly(ADP-ribose) polymerase inhibition: a new direction for BRCA and triple-negative breast cancer? *Breast Cancer Res*., **13**, 218.
59. Turner,N.C. *et al.* (2008) A synthetic lethal siRNA screen identifying genes mediating sensitivity to a PARP inhibitor. *EMBO J*., **27**, 1368–1377.
60. Sahu,R.P. *et al.* (2009) Activation of ATM/Chk1 by curcumin causes cell cycle arrest and apoptosis in human pancreatic cancer cells. *Br. J. Cancer*, **100**, 1425–1433.
61. Wang,W.Z. *et al.* (2008) Abrogation of G2/M arrest sensitizes curcumin-resistant hepatoma cells to apoptosis. *FEBS Lett*., **582**, 2689–2695.
62. Annunziata,C.M. *et al.* (2010) Poly (ADP-ribose) polymerase as a novel therapeutic target in cancer. *Clin. Cancer Res*., **16**, 4517–4526.
63. Simbulan-Rosenthal,C.M. *et al.* (2003) PARP-1 binds E2F-1 independently of its DNA binding and catalytic domains, and acts as a novel coactivator of E2F-1-mediated transcription during re-entry of quiescent cells into S phase. *Oncogene*, **22**, 8460–8471.
64. Verlinden,L. *et al.* (2007) The E2F-regulated gene Chk1 is highly expressed in triple-negative estrogen receptor/progesterone receptor/HER-2 breast carcinomas. *Cancer Res*., **67**, 6574–6581.
65. Bindra,R.S. *et al.* (2007) Repression of RAD51 gene expression by E2F4/p130 complexes in hypoxia. *Oncogene*, **26**, 2048–2057.
66. Toledo,L.I. *et al.* (2011) A cell-based screen identifies ATR inhibitors with synthetic lethal properties for cancer-associated mutations. *Nat. Struct. Mol. Biol*., **18**, 721–727.
67. Reaper,P.M. *et al.* (2011) Selective killing of ATM- or p53-deficient cancer cells through inhibition of ATR. *Nat. Chem. Biol*., **7**, 428–430.

Received February 14, 2013; revised June 12, 2013; accepted June 30, 2013